Agricultural and Forest Meteorology 182–183 (2013) 156–167

Contents lists available at ScienceDirect

Agricultural and Forest Meteorology

journal homepage: www.elsevier.com/locate/agrformet

Carbon dynamics in the Amazonian Basin: Integration of eddy covariance and ecophysiological data with a land surface model

Bassil El-Masri*, Rahul Barman, Prasanth Meiyappan, Yang Song, Miaoling Liang[1], Atul K. Jain

Department of Atmospheric Sciences, University of Illinois at Urbana-Champaign, Urbana, IL, United States

ARTICLE INFO

Article history:
Received 13 August 2012
Received in revised form 27 February 2013
Accepted 27 March 2013

Keywords:
ISAM
GPP
NPP
Soil carbon
LBA

ABSTRACT

Information contained in eddy covariance flux tower data has multiple uses for the development and application of global land surface models, such as evaluation/validation, calibration and process parameterization for carbon stocks and fluxes. In this study, we combine Large Scale Biosphere–Atmosphere Experiment in Amazonia (LBA) project data collected from a network of eddy covariance flux towers deployed across the Amazonian basin to improve the carbon stocks and flux estimated by a land surface model, the Integrated Science Assessment Model (ISAM). We evaluate the key model parameters for carbon allocation factors, maintenance respiration as well as the autotrophic respiration using the LBA site measurements. Our model results show that the total biomass ranges from 0.7 $\mathrm{kg\,C\,m^{-2}\,yr^{-1}}$ for the pasture site to 20.8 $\mathrm{kg\,C\,m^{-2}\,yr^{-1}}$ for the forest site. The ISAM estimates for GPP and NPP are well within the uncertainty range of the site measurement data. Also, the results revealed that all, but one forest site have lower net primary productivity (NPP) to gross primary productivity (GPP) ratio (NPP/GPP = 0.4 compared to the savanna and the pasture sites (NPP/GPP = 0.5). This is because savanna and the pasture sites experienced the longest dry season and plants growing in such environmental conditions have stronger efficiency to store carbon compared to forests. The forest evergreen site (Km67) has a higher measured NPP/GPP ratio (0.5), because of higher carbon accumulation. Soil carbon is lowest for the pasture site (Km77) (7.2 $\mathrm{kg\,C\,m^{-2}\,yr^{-1}}$) and highest for the forest site (Km34) (12.8 $\mathrm{kg\,C\,m^{-2}\,yr^{-1}}$). The model results suggest that all the forest sites are a net sink for atmospheric CO_2, while the savanna (PDG) and pasture (FNS) sites are neutral and another pasture site (Km77) is net source for atmospheric CO_2. Meanwhile, the model results highlight the importance of the LBA site data to improve the model performance for the tropical Amazon region. The study also suggest the need for a network of long-term monitoring plans to measure changes in the vegetation and soil carbon biomass at the local and regional levels. Such programs will be necessary to make reliable global carbon emissions estimates.

1. Introduction

The Amazonian forests play a key role in the global carbon cycle, contributing to about 30% of the global biomass and terrestrial productivity (Beer et al., 2010; Houghton et al., 2001; Malhi and Grace, 2000; Melillo et al., 1996). The increase in air temperature, and shift in precipitation intensity and duration due to climate change has altered carbon fluxes from the Amazonian rainforests (Botta et al., 2002). Some studies suggested that CO_2 fertilization might have led to an increase in carbon uptake by about 3 $\mathrm{Pg\,C\,yr^{-1}}$ in undisturbed forests (Houghton et al., 2000; Saleska et al., 2003). In contrast, ecosystem modeling studies suggest that due to climate variability, the Amazon basin is a net source during the drier and warmer El Niño and net sink during the wetter and cooler La Niña cycle (Asner et al., 2000; Baker et al., 2008; Foley et al., 2002; Potter et al., 2001, 2009; Tian et al., 1998).

The landscape of Amazon is also changing dramatically due to human activities. Over the past few decades, increased demand for agricultural products due to rising population led to massive deforestation rates (Asner et al., 2005; Moran, 1993; Morton et al., 2005; Skole and Tucker, 1993). Deforestation can also lead to degradation in the ecosystem services such as lower water quality, spread of infectious diseases, and increases in tree mortality through an increase in fire frequency (Foley et al., 2007). It is expected that the rates of deforestation will continue to increase as more urbanization expands to the core of the forest (Laurance et al., 2001). Such

---

* Corresponding author. Tel.: +1 2173001842.
E-mail addresses: belmasri@illinois.edu (B. El-Masri), rbarman2@illinois.edu (R. Barman), meiyapp2@illinois.edu (P. Meiyappan), song81@illinois.edu (Y. Song), mliang@Princeton.edu (M. Liang), jain1@illinois.edu (A.K. Jain).

[1] Current address: Civil and Environmental Engineering, Princeton University, Princeton, NJ, United States.

0168-1923/$ – see front matter © 2013 Elsevier B.V. All rights reserved.
http://dx.doi.org/10.1016/j.agrformet.2013.03.011

Notation

Veg_frct	vegetation cover fraction
$\mathrm{Cn}_{\mathrm{leaf}}$	carbon:nitrogen ratio for the leaves
$\mathrm{Cn}_{\mathrm{stem}}$	carbon:nitrogen ratio for the stem
$\mathrm{Cn}_{\mathrm{roots}}$	carbon:nitrogen ratio for the roots
V_{cmax}	maximum carboxylation rate at 25 °C
k_n	light extinction coefficient
k_{leaf}	base respiration rate for leaves
K_{stem}	base respiration rate for stem
K_{root}	base respiration rate for roots
ω	allocation parameter
$\varepsilon_{\mathrm{leaf}}$	parameter controlling allocation to leaves
$\varepsilon_{\mathrm{stem}}$	parameter controlling allocation to stem
$\varepsilon_{\mathrm{root}}$	parameter controlling allocation to roots
k	allocation parameter
Y_{leaf}	leaf life span
r_{wmax}	maximum drought leaf loss rate
r_{tmax}	maximum cold leaf loss rate
b_w	parameter for leaf loss (drought)
b_t	parameter for leaf loss (cold)
T_{cold}	temperature threshold for leaf loss because of cold stess
Y_{stem}	stem turnover rate
Y_{froot}	fine root turnover rate
Y_{croot}	coarse root turnover rate
R_{leaf}	maintenance respiration for leaves
R_{stem}	maintenance respiration for stem
R_{root}	maintenance respiration for roots
R_{mtotal}	total maintenance respiration
R_G	growth respiration
R_{auto}	autotrophic respiration
C_{leaf}	leaf carbon
C_{stem}	stem carbon
C_{root}	root carbon
Ø	leaf phonological status defined as the current fraction of maximum LAI
gt	temperature dependent function
T_{veg}	vegetation temperature (°C)
T_{soil}	soil temperature (°C)
GPP	gross primary productivity
NPP	net primary productivity
$\mathrm{Allo\_fact}_{\mathrm{leaf}}$	allocation factor for leaves
$\mathrm{Allo\_fact}_{\mathrm{stem}}$	allocation factor for stem
$\mathrm{Allo\_fact}_{\mathrm{root}}$	allocation factor for roots
L	light availability factor
ws	water stress factor
LAI	leaf area index
LAI_max	biome specific maximum LAI
T_r	root temperature
Bio_tr	biome specific root temperature
Bio_trmin	biome specific minimum root temperature
daylen	biome specific day length

rapid changes in land use will lead to a massive carbon release from the soils, and vegetation speeding up the climate change. The forests and woodlands (e.g. Savannas) also exchange large amounts of water and energy with the atmosphere, and the loss of large areas of Amazonian forest due to land-use and land-use change could impact local and regional climates (Ramankutty et al., 2007).

Given the importance of the Amazon basin toward the regional and global budgets of carbon, energy, and water fluxes (Andreae et al., 2002; Costa and Foley, 2000; Foley et al., 2007; Werth and Avissar, 2002), an international scientific endeavor headed by Brazil had led to the establishment of a Large Scale Biosphere-Atmosphere Experiment in Amazonia (LBA) (Avissar and Nobre, 2002) The main science objective of the LBA project is to understand the interactions between the atmosphere and climate change variability, in the Amazonian terrestrial ecosystems (Avissar et al., 2002). Such observational data from the LBA sites can substantially improve the understanding of the carbon exchange between the terrestrial ecosystem and the atmosphere and the detection of deficiencies in the land surface models (LSMs). For instance, several studies using LSMs have predicted a decline in topical forest water and carbon fluxes during the dry season (Botta et al., 2002; Tian et al., 1998), while site measurements suggest the opposite (Von Randow et al., 2004; Saleska et al., 2003). Without constraining the models using site observations, LSMs would perhaps underestimate the global carbon fluxes and fail to detect the carbon dynamic of the tropical forests (Saleska et al., 2003). Therefore, these observations are crucial for the improvement of LSMs. Since climate change and variability affect the global terrestrial biogeophysical and biogeochemical cycles (Davidson et al., 2012; Malhi et al., 2008), LSMs with their complex and detailed biogeochemical and biogeophysical processes are important tools to gain better understanding of the interactions between the Amazon basin terrestrial ecosystem and environmental change.

In this paper, we take advantage of observational data from flux tower sites to present a methodology to calibrate and improve an LSM by identifying and modifying the key model carbon schemes in order to enhance the vegetation and the soil carbon estimates. We use the Integrated Science Assessment Model (ISAM) to show the feasibility of our approach and its relevance to other LSMs. This paper extends upon previous modeling application of the ISAM (Jain et al., 2009; Yang et al., 2009) by detailing the carbon dynamics of the LBA sites representing forests, savannas, and pastures ecosystems of the Amazonian basin. Notably, the version of ISAM used in this study contains detailed biogeophysical processes (Song et al., 2013) coupled into the biogeochemical component of ISAM. This extended version of the model is used to examine the interannual variability of carbon fluxes (Gross primary production (GPP), net primary production (NPP), autotrophic and heterotrophic respirations) and above and below ground biomass of eight LBA study sites in the Amazon basin (Table 1). The objective has been achieved by comparing the model estimated carbon fluxes with eight LBA project flux towers measurements. The study is designed to: (1) provide a brief description of the carbon dynamics of ISAM, (2) calibrate the model parameters using site data, (3) evaluate the model performance by comparing the model calculated carbon fluxes with eddy covariance flux towers measurements, and (4) evaluate the model estimated soil and vegetation carbon with published studies.

2. Methodology

2.1. ISAM description

The ISAM is one of the 23 models participating in the LBA project to study the responses of Amazon basin terrestrial ecosystems to environmental factors. The ISAM is a land surface model that is applied to examine the impacts of changing CO_2 in the atmosphere, fire, and land use change on terrestrial ecosystems functions (Jain et al., 1996; Jain and Yang, 2005; Jain et al., 2006). ISAM has also been used to describe the dynamic of the terrestrial biosphere carbon (Jain et al., 1996; Jain and Yang, 2005) and nitrogen (Jain et al., 2009; Yang et al., 2009). It was a part of the IPCC assessments of future climate change scenarios (Schimel et al., 1996; Prentice et al., 2001). The latest version of the ISAM has also participated in the Modeling and Synthesis Thematic Data Center (MAST-DC) study as

Table 1
List of the eddy flux tower sites used in this study.

Site name	Biome type	Lat (°S)	Lon (°W)	Canopy height (m)	Climate	Years	Reference
Manaus (Km34)	Evergreen broadleaf forest	2.61	60.21	35	Dry season: July–September	2002–2005	Araújo et al. (2002)
Santarém (Km67)	Evergreen broadleaf forest	2.86	54.96	55	Dry season: July–November	2002–2004	Hutyra et al. (2007)
Santarém (Km83)	Evergreen broadleaf forest	3.02	54.97	35	Dry season: July–November	2001–2003	Da Rocha et al. (2004), Miller et al. (2004)
Reserva Jarú (RJA)	Evergreen broadleaf forest	10.08	61.93	35	Dry season: June–August	2000–2002	Von Randow et al. (2004)
Javaes River - Bananal Island (BAN)	Semi deciduous forest	9.82	50.16	16	Dry season: May–September	2004–2006	Borma et al. (2009)
Reserva Pe-de-Gigante (PDG)	Woody savanna	21.62	62.36	10	Dry season: April–September	2002–2003	Da Rocha et al. (2002)
Fazenda Nossa Senhora (FNS)	Pasture	10.76	62.36	0.5	Dry season: May–September	1999–2001	Andreae et al. (2002), Von Randow et al. (2004)
Santarém (Km77)	Pasture	3.02	54.89	0.6	Dry season: July–December	2001	Sakai et al. (2004)

part of the North American Carbon Program (NACP) to quantify and understand spatial and temporal distributions of carbon sources, sinks, and inventories by synthesizing NACP data and models, from sites to regional/continental scales (Huntzinger et al., 2012; Keenan et al., 2012; Richardson et al., 2012; Schaefer et al., 2012).

The land component of the ISAM used in this study simulates carbon, nitrogen, energy, and water fluxes at 0.5° × 0.5° spatial resolution and at multiple temporal resolutions ranging from half hourly to yearly. The ISAM has two main components: (1) a biogeochemical module where soil carbon, litter production, respiration, productivity, carbon, and stocks for different vegetation pools are estimated (Fig. 1) (Jain et al., 1996; Jain and Yang, 2005; Yang et al., 2009) and (2) a biogeophysical module representing sunlit-shaded photosynthesis schemes (Dai et al., 2004), energy, and soil/snow hydrology (Song et al., 2013; Oleson et al., 2008; Lawrence et al., 2011). In addition, ISAM biogeochemistry has a dynamic nitrogen cycle module that estimates nitrification, denitrification, leaching, and volatilization as well as nitrogen limitations on plant productivity (Fig. 1) (Yang et al., 2009; Jain et al., 2009).

The ISAM is composed of seven vegetation pools and eight litter and SOM pools (Fig. 1). Each grid cell is occupied by at least one of the twenty eight managed or unmanaged land cove types (primary and secondary forests, C3 and C4 grasses, C3 and C4 croplands, C3 and C4 pastures, shrubland, tundra, urban), and bare ground as described in Meiyappan and Jain (2012).

The ISAM utilizes Farquhar et al. (1980) C3 photosynthesis model as implemented by Collatz et al. (1991), and the Collatz et al. (1992) C4 photosynthesis model. The stomatal conductance model is a variant of the Ball-Berry stomatal conductance model (Ball et al., 1987; Collatz et al., 1991). The ISAM computes stomatal conductance and photosynthesis for sun and shaded leaves where leaf area index (LAI) is used to scale those variables from the leaf to the canopy level. GPP is modified through the feedback of nitrogen availability on carbon assimilation, and is obtained by dynamically comparing plant nitrogen demand and supply (McGuire et al., 1992).

GPP is allocated to leaves and the leaf NPP (GPP minus leaf maintenance and growth respirations) is allocated to stem, and roots. Maintenance respiration is calculated separately for leaves, stem, and root (coarse and fine) based on Sitch et al. (2003) and a temperature dependent Q_{10} factor (Arora, 2003). The growth respiration for each pool is assumed to be a fixed percentage (25%) of the difference between GPP and maintenance respiration (Sitch et al., 2003). Equations describing carbon allocation, maintenance respiration, and phenology key processes that determine NPP, litter production, autotrophic respiration, and above and below ground biomass have not yet been documented, and hence the equations describing these fluxes in the ISAM are given in Appendix A.

The phenology implemented in the ISAM is based on Arora and Boer (2005) and White et al. (1997), with some modifications to include a water stress factor that triggers senescence for herbaceous biomes (White et al., 1997) and the use of minimum LAI to indicate the start of the leaf fall period. The phenology for deciduous forest ecosystems has four stages: leaf onset which indicates the start of the growing season, normal growth, leaf fall, and a dormant, which indicates no leaf presence (Table A2 of the appendix). The evergreen forests are always on normal growth. The herbaceous biomes have three phonological stages during their growth, which are the same as the first three phenology stages of the deciduous forests. Unlike deciduous forests, herbaceous ecosystems do not enter the dormant stage and they maintain leaves as long as the environmental conditions permit. The transition from one stage of the phenology to another is triggered when certain environmental and physiological conditions are met (Arora and Boer, 2005).

Allocation to and from the eight vegetation pools produces dynamic vegetation that in turn produces litter fall and SOC. The

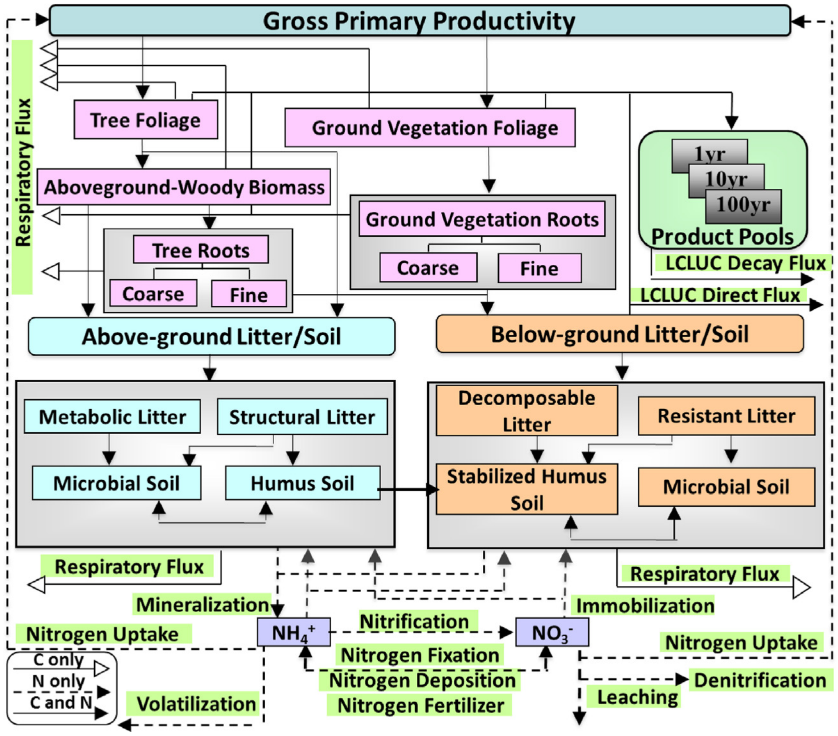

Fig. 1. Schematic diagram of all reservoirs and flows of carbon and nitrogen in the ISAM.

allocation of carbon to the seven vegetation pools is dependent on light, water and phenology stages of the canopy and follows the formulations of Friedlingstein et al. (1999) and Arora and Boer (2005) (see Appendix A), where during leaf onset carbon is allocated only to the leaves. During normal leaf growth, carbon is allocated to the seven vegetation carbon pools and it ceases to the leaves during leaf fall. The allocation of carbon to the vegetation pools is constrained due to adverse effects of limited availability of light, water, and nitrogen. Accordingly, the allocation in roots can help address the limited availability of water and nitrogen, while investments in stems tend to increase access to light.

The carbon allocation process is constrained by three conditions. First, for the cold deciduous trees all carbon is allocated only to the leaves during leaf onset. A second condition is that sufficient woody biomass must be available to support the mass of leaves. A third condition is to assure that the plant structure is preserved, meaning sufficient root and stem biomass must be built prior to support the leaf biomass.

The model estimates litter fall from leaves, stem and roots, which is a function of temperature, water stress, and turnover rates. The turnover time scale for leaves is biome dependent and varies from 0.75 year for savanna to 2 years for evergreen forest (Foley et al., 1996). The turnover rates for the stem vary from 2.5 years for savanna to 50 years for evergreen forest (Malhi et al., 2004) and, between 1 and 8 years for the roots.

2.2. Model calibration and spin-up

In this study, we use data from eight LBA flux tower sites: covering four tropical evergreen forest sites, one tropical deciduous forest, one savanna, one pasture, and one pasture/agricultural site (Table 1). The Santarém Km77 was originally a pasture site from September 2000 until November 2001, but was converted to a rice site in February 2002 (Sakai et al., 2004). We simulate this site as a pasture (January 2001–November 2001), discontinuing .the model calculations after November 2001 because the flux measurements are available until that month. The Javaes River–Bananal Island (BAN) site is a semi-deciduous site and it resembles the features of evergreen forests. Hence, we treat this site as tropical evergreen site similar to other modeling studies (e.g. Poulter et al., 2010). The readers are referred to de Gonçalves et al. (2012) for details about the site used in this study.

To improve the model estimated carbon pool sizes and fluxes for tropical forest sites, the carbon allocation factors and the maintenance respiration rates (values are provided in the appendix) are calibrated based on LBA site data. Following Malhi et al. (2011), the allocation factors are adjusted to have 35% of the carbon allocated each to the stem and leaf pools and 30% to the roots pools. The calibrated allocation factors are dynamic and their values can change with time depending on water and light stress factors (Arora and Boer, 2005). Studies suggest that maintenance respiration rates are different for different carbon pools (Amthor, 1984, 2000; Ryan et al., 1995). Therefore, different maintenance respiration rates for leaf, stem, and, root pools for each biome are introduced in the maintenance respiration equations (Table S2).

The ISAM parameters for carbon allocation, maintenance respiration, and turnover rates are parameterized using the measured data from tropical biome site Km34. We optimize the model by using trial and error method to find parameters that can achieve the minimum absolute difference between the observed and the estimated variables. The optimization is done for each biome type because the parameters are biome specific. In addition, measured parameters that are available from the literature are used directly without optimization. We evaluate the optimized model using four other tropical sites (Km67, Km83, RJA, and BAN). Similarly, we calibrate the above mentioned model parameters for the FNS pasture site and tested the model using the other pasture site Km77. Also, we run and evaluate the model performance for a woody savanna site PDG. We could not validate it with other LBA savanna sites, due to the lack of data. However, we compare our model results with other published measured studies (Grace et al., 2006). Finally, we also evaluate and compare our model results with site

Table 2
Summary of ISAM estimated aboveground and belowground carbon (Kg C m^{-2} yr^{-1}) reported as the mean for the study sites flux measurement period.

		Km34	Km67	Km83	RJA	BAN	PDG	FNS	Km77
C_{leaf}	ISAM	0.7	0.6	0.7	0.6	0.6	0.4	0.2	0.1
	Measurement	–	–	–	–	–	0.2–0.4[f]	–	–
C_{stem}	ISAM	17.2	12.6	16.9	16.2	14.7	0.5	–	–
	Measurement	–	–	–	–	–	0.7–1.2[f]	–	–
C_{root}	ISAM	2.9	2.2	2.8	2.7	2.4	1.0	1.2	0.6
	Measurement	–	–	–	–	–	–	–	–
AGB	ISAM	17.9	13.2	17.6	16.8	15.3	0.9	0.2	0.1
	Measurement	16.5 ± 5[a]	14.8 ± 3[a]	15.6[b] 18.5–20.4[c]	–	–	–	–	–
BGB	ISAM	2.9	2.2	2.8	2.7	2.4	1.0	1.2	0.6
	Measurement	3.8 ± 0.6[a]	1.8 ± 0.7[b]	–	–	–	0.7–1.1[d]	–	–
Total Biomass	ISAM	20.8	16.4	20.4	19.5	17.7	1.9	1.4	0.7
	Measurement	20.3 ± 5.6[a]	16.6 ± 3.6[a]	19.9–21.8 ± 0.2[a]	–	–	1.7–2.3[e]	–	–

[a] Measurements data are from Malhi et al. (2009), unless indicated by a letter.
[b] Measurement from Saleska et al. (2003).
[c] Measurement from Miller et al. (2004).
[d] Measurement from De Castro and Kaufman (1998).
[e] Measurement from Da Rocha et al. (2002).
[f] Measurements from Grace et al. (2006).

ecophysiological measurements for NPP, autotrophic respiration, heterotrophic respiration, biomass, soil carbon, and leaf litter.

The model is initialized using site level soil properties and site meteorological data and with the absence of CO_2 and nitrogen disturbance. The spin-up is achieved by repeating the site meteorological data for the range of available years until the carbon and nitrogen pools reach the steady state, which takes about 700 years for the soil carbon. Next, the model is run for each site for the site measurement period.

3. Results

This study uses a network of meteorological and climate data from Amazon sites to drive the ISAM to calculate and compare the carbon fluxes with relevant observations of ecosystem fluxes. Specifically, this study takes advantage of the LBA project updated database from eight flux towers across a gradient of ecosystems within Amazon. The ISAM systematically calculates carbon fluxes and storage in the Amazon vegetation and soils.

3.1. *Biomass*

The ISAM calculated aboveground biomass (AGB) ranges between 0.2 kg C m^{-2} yr^{-1} for pasture and 17.9 kg C m^{-2} yr^{-1} for tropical evergreen forest (Table 2). The AGB for the Km34, the Km67, and the Km83 sites are within the range of the site measured data. There are no measured data available for AGB for the RJA and BAN tropical evergreen sites, but the ISAM estimated AGB for this site falls within the range of Km34 and the Km67 sites (Table 3). The pasture (FNS and Km77) and the savanna (PDG) sites store more carbon in the roots (C_{root}) than in the above ground and range from 0.7 to 1.2 kg C m^{-2} yr^{-1} (Table 2). Below ground biomass (BGB) for the Km34 and Km67 sites is estimated to be between 2.2 and 2.9 kg C m^{-2} yr^{-1} with BGB for the Km34 site being slightly lower than the measured value (Table 3). As expected, carbon in forest ecosystems is mostly stored in the stem (C_{stem}), whereas for grassland in the roots (Fig. 2). On the other hand, ISAM estimated total biomass for the Km83 site (20.4 kg C m^{-2} yr^{-1}) was within the range of measured total biomass (Table 2). The ISAM modeled total biomass for the other tropical sites ranges from 16.4 to 20.8 kg C m^{-2} yr^{-1}, which is within the measured range of values of total biomass at the Km34, Km67 and Km83 sites (Table 3). The modeled total biomass for the savanna (PDG) site is 1.9 kg C m^{-2} yr^{-1}, which falls within the measured value of total biomass, while total biomass for the pasture sites (FNS and Km77) are 1.4 and 0.9 kg C m^{-2} yr^{-1} (Table 2), respectively. The variation

Table 3
ISAM estimated soil carbon (Kg C m^{-2}) for the LBA study sites reported as the mean for the study sites flux measurement period.

	Soil carbon (0–1 m)	
	ISAM	Measurement
Km34	12.8	12.7[a]
Km67	12.6	12.0[a]
Km83	12.2	7.8 ± 1.1–11.2 ± 1.3[b]
RJA	10.0	–
BAN	10.2	–
PDG	8.3	8.3–8.9[c]
FNS	10.3	10.0–12.0[c] 10.0-10.8[d]
Km77	7.2	–

[a] Measurements are from Malhi et al. (2009).
[b] Measurements are from De carvalho Conceição Telles et al. (2003) for 1 m soil depth.
[c] Measurements are from Fishers et al. (1994) for Savanna and pasture sites in Colombia.
[d] Measurements are from Trumbore et al. (1995).

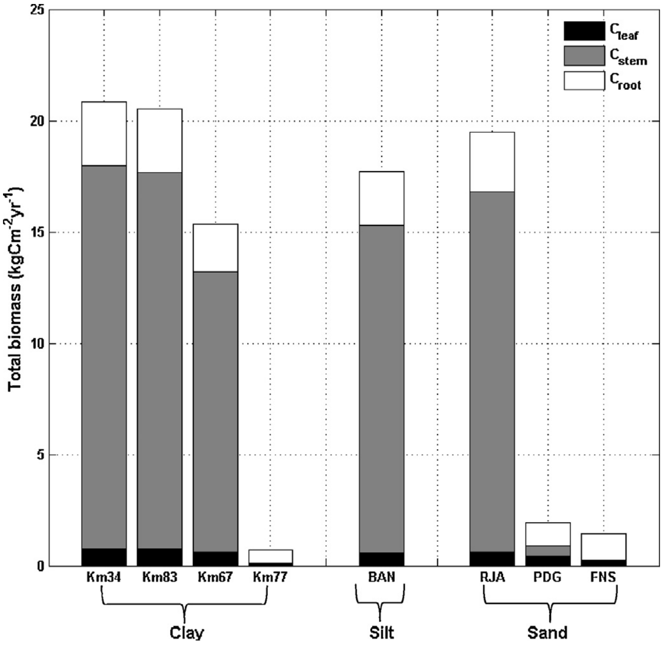

Fig. 2. Component of total biomass for each site in kg C m^{-2} yr^{-1} grouped with respect to soil types.

in the total biomass for the tropical evergreen sites is due to the fact that the soil characteristics vary with site. The sites with clay soil have higher biomass than the sites with silt or sandy soils. However, the topical evergreen site Km67 is exceptional, which has been disturbed over the time and therefore has lower total biomass compared to other LBA forest sites (Fig. 2).

3.2. Soil carbon

The model estimated soil carbon for the top1 m soil depth ranges between 7.2 kg C m^{-2} (Km77 site) and 12.8 kg C m^{-2} (Km34 site) (Table 3). The ISAM estimated soil carbon for the Km67 site is only 4.5% higher than the site measurement. The soil carbon estimates for the RJA and BAN forest sites are within the range of the site measurement for Km83. The estimated soil carbon for the savanna site (PDG) is at the lower end of the site measurement. The estimated soil carbon for the pasture site (FNS) (10.3 kg C m^{-2}) is higher than that of the savanna site, but the model estimated soil carbon for both of these sites are within the range of measured soil carbon (Table 3). The pasture site (Km77) soil carbon (7.2 Kg C m^{-2}) is lower than the other pasture site (FNS) which can be related to difference in soil types and textures (Andreae et al., 2002; Keller et al., 2005) that determines the amount of carbon stored in the soil.

3.3. GPP

Overall, the ISAM GPP results are in good agreement with measurements (Table 4). For tropical evergreen sites, model estimated GPP vary between 2.6 and 3.0 kg C m^{-2} yr^{-1} compared to flux tower measured values of 2.7–3.1 kg C m^{-2} yr^{-1} (Table 4). The GPP for the savanna and pasture sites are lower than the forest sites, because herbaceous ecosystems are less productive than forest ecosystems. The ISAM estimated GPP for the individual sites is within 15% of flux measurement values. When considering the large uncertainties in the measured flux GPP (±5–20%) that are related to errors in the partitioning of net ecosystem exchange (NEE) into ecosystem respiration and GPP and errors in energy balance closer (Hollinger and Richardson, 2005; Wilson et al., 2002), the model GPP estimates are within the uncertainty range of the measured flux GPP values.

The GPP for the FNS pasture site is about 3 times higher than the other pasture site (km77). One explanation for the large difference in productivity between these two pasture sites is that the productivity of the Km77 site is lower due to water and nutrient stresses (Sakai et al., 2004). Therefore, Km77 site LAI is almost half of that of the FNS site LAI.

To evaluate the model performance for the yearly changes in GPP, we compared the estimated GPP with site measurements. The model performances for all, but pasture site (FNS) for year 2001 are compared well with the measurements for all the measured years (Fig. 3). While exact cause of underestimation of GPP for the FNS pasture site GPP for year 2001 is unknown; we speculate this could be due to errors in some measured input variable.

3.4. Respiration

The ISAM estimated maintenance respiration for the leaf (R_{leaf}) (0.4–0.7 kg C m^{-2} yr^{-1}), stem (R_{stem}) (0.3–0.4 kg C m^{-2} yr^{-1}), and roots (R_{root}) (0.3–0.4 kg C m^{-2} yr^{-1}) for tropical evergreen sites are within the range of measured values (Table 4). Leaf maintenance respiration rates are higher than stem and roots because of the high leaf turnover rates (0.75–2 years for the leaves compared to 1–50 years for roots and stem; Table A1). The model estimated R_{leaf} is lower for the savanna (PDG) and the pasture (FNS) sites than the forest sites because of lower LAI (data not shown) and leaf carbon (Table 4).

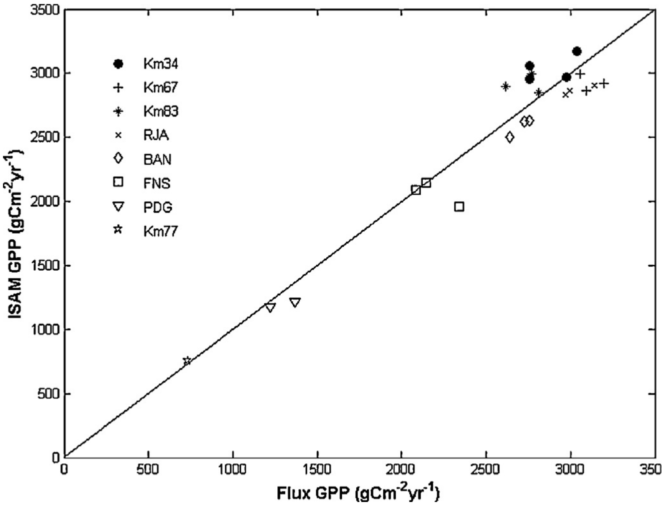

Fig. 3. Scatter plot for the relationship between ISAM estimated GPP and flux GPP per year for each site in g C m^{-2} yr^{-1}. The solid line represents the 1:1 line.

Similarly, the ISAM estimated autotrophic respiration (R_{auto}) (the sum of leaf, stem, roots, and growth respiration) for the tropical evergreen sites vary between 1.5 and 2.0 kg C m^{-2} yr^{-1}, which fall within the range of measured R_{auto} for the Km34 and the Km67 sites (Table 4). The savanna (PDG) site and the pasture site (Km77) have the lowest R_{auto} (0.5 kg C m^{-2} yr^{-1}), while pasture (FNS) site R_{auto} (1.0 kg C m^{-2} yr^{-1}) is almost half of the forest sites, which could be attributed to lower GPP compared to the evergreen sites (Table 4). R_{leaf} for the tropical evergreen sites is about third of the total R_{auto} (Fig. 4). The R_{root} for the pasture sites (FNS) is the highest, which is about 50% of the total R_{auto}, while R_{leaf} leaf respiration accounts for about 10% of the total R_{auto} (Fig. 4). The model is able to capture the variability in the maintenance respiration for each of the vegetation pool of forest and herbaceous biomes. Model results show that the herbaceous sites (especially for the pasture sites) have higher R_{root}, whereas for the forest biomes R_{leaf} is the highest (Table 4).

The simulated soil respiration (R_{hetro}) estimates for the tropical evergreen forests (0.9–1.1 kg C m^{-2} yr^{-1}) are also within the range of measured values (Table 4), except for the Km67 site. The ISAM estimated R_{hetro} for Km67 is lower than the measured fluxes, while leaf, stem, root respiration and the R_{auto} are within the range of

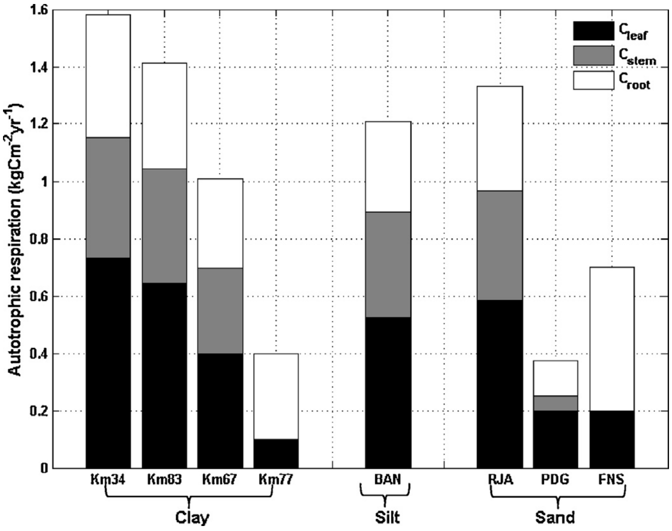

Fig. 4. Component of autotrophic respiration for each site in kg C m^{-2} yr^{-1} grouped with respect to soil types.

Table 4
Summary of ISAM estimated carbon fluxes (Kg C m^{-2} yr^{-1}) reported as the mean for the study sites flux measurement period. Measurements for GPP are from eddy flux tower measurements; while the remaining variables are ecophysiological measurements from Malhi et al. (2009).

		Km34	Km67	Km83	RJA	BAN	PDG	FNS	Km77
GPP	ISAM	3.0	2.9	2.9	2.9	2.6	1.2	2.1	0.8
	Measurement	2.9	3.1	2.7	3.0	2.7	1.3	2.2	0.7
NPP	ISAM	1.1	1.4	1.1	1.1	1.0	0.6	1.1	0.4
	Measurement	1.0 ± 0.1	1.4 ± 0.1	–	–	–	–	–	–
R_{auto}	ISAM	2.0	1.5	1.8	1.7	1.5	0.6	1.0	0.4
	Measurement	2.0 ± 0.5	1.5 ± 0.4	–	–	–	–	–	
R_{leaf}	ISAM	0.7	0.4	0.6	0.6	0.5	0.2	0.2	0.1
	Measurement	1.0 ± 0.4	0.7 ± 0.4	–	–	–	–	–	–
R_{stem}	ISAM	0.4	0.3	0.4	0.4	0.4	0.05	–	–
	Measurement	0.4 ± 0.1	0.4 ± 0.1	–	–	–	–	–	–
R_{root}	ISAM	0.4	0.3	0.4	0.4	0.3	0.1	0.5	0.3
	Measurement	0.5 ± 0.2	0.4 ± 0.8	–	–	–	–	–	–
R_{hetro}	ISAM	1.1	1.0	1.0	1.0	0.9	0.6	1.0	0.6
	Measurement	1.0 ± 0.1	1.5 ± 0.1	–	–	–	–	–	–
R_{total}	ISAM	3.1	2.5	2.8	2.7	2.4	1.2	2.0	1.0
	Measurement	2.9 ± 0.5	3.0 ± 0.4		–	–	–	–	–
NEE	ISAM	−0.1	0.4	0.1	0.2	0.2	0.0	0.1	-0.2
	Measurement	0.5 ± 0.2[a] 1.4 ± 3.8[b]	0.5 ± 0.1[a] −1.1[b]	–		–	–	–	–
NPP/GPP	ISAM	0.4	0.5	0.4	0.4	0.4	0.5	0.5	0.5
	Measurement	0.34	0.5	–	–	–	–	–	–

[a] Ecophysiological measurements.
[b] Gas exchange measurements.

site measurements. It is hypothesized that the Km67 site has experienced mortality disturbance (Malhi et al., 2009; Saleska et al., 2003), but this disturbance has not been quantified in the literature (Marcos Costa, pers. comm.). The inability to determine the right disturbance history over the measured time hinders the model ability to estimate R_{hetro}, because R_{hetro} is expected to increase following disturbance due to increased microbial respiration with vegetation growth (Concilio et al., 2006; Vargas and Allen, 2008).

The R_{total} for the tropical evergreen site, Km34 (3.1 kg C m^{-2} yr^{-1}) is very similar to the measured R_{total}. There are no measured data available for the other forest sites, but the model estimated R_{total} is close to the measured values at Km34 and Km67 sites (Table 4). The ISAM estimated R_{total} for the savanna (PDG) and the pasture (FNS and Km77) sites are lower than the forest sites mainly because of lower R_{auto} for these two sites (Table 4). Examining the component (R_{auto} and R_{hetro}) of total respiration, the ISAM estimated R_{auto} is about two third of the R_{total} for tropical evergreen sites and about half for the savanna (PDG) and the pasture (FNS and Km77) sites (Fig. 5), which are consistent with the measurement data.

3.5. NPP

The ISAM NPP estimates for tropical evergreen forest varies between 1.0 and 1.4 kg C m^{-2} yr^{-1} which falls within the range of reported NPP values for the same biome (Table 4). The model estimated NPP for deciduous forest (BAN), savanna (PDG) and the two pasture sites (FNS and Km77) are 1.0, 0.6, 1.1, and 0.4 kg C m^{-2} yr^{-1}, respectively (Table 4).

3.6. NPP: GPP ratio

The model estimated forest carbon use efficiency (NPP/GPP ratio) varies from 0.4 to 0.5 for the tropical evergreen sites, which is similar to the measured NPP/GPP ratio of 0.34 (for the Km34) and 0.5 (for the Km67). The Km67 site has a higher measured NPP/GPP ratio (0.5) compared to other tropical evergreen sites, which suggest that this tropical evergreen site is accumulating more carbon than the other LBA tropical evergreen sites. Malhi et al. (2009) suggest that the enhanced NPP for the Km67 site is due to a shift in carbon allocation to wood production because GPP is similar to the other tropical evergreen forest sites. The savanna (PDG) and the pasture (FNS and Km77) sites have higher NPP/GPP ratio of 0.5 (Table 4) mainly because of lower GPP and R_{auto}. Moreover, the savanna and the pasture sites experience the longest dry season and plants growing in such environmental conditions have stronger efficiency to store carbon as they have less plant material to sustain compared to forests (Zhang et al., 2009). Also, the transition from dry to wet climate leads to an increase in plant respiration which may cause a decrease in NPP.

3.7. Leaf litter

The modeled leaf litter is close to the measurements except for the Km67 site and range from 0.2 kg C m^{-2} yr^{-1} to 0.3 kg C m^{-2} yr^{-1} (Table 5). The leaf litter for the pasture site (FNS) (0.2 kg C m^{-2} yr^{-1}) is at the higher end of the reported measurements, while for the other pasture site (Km77) the value (0.1 kg C m^{-2} yr^{-1}) is at the lower end of the reported measurements. The difference between the model estimated leaf litter for the two pasture sites can be

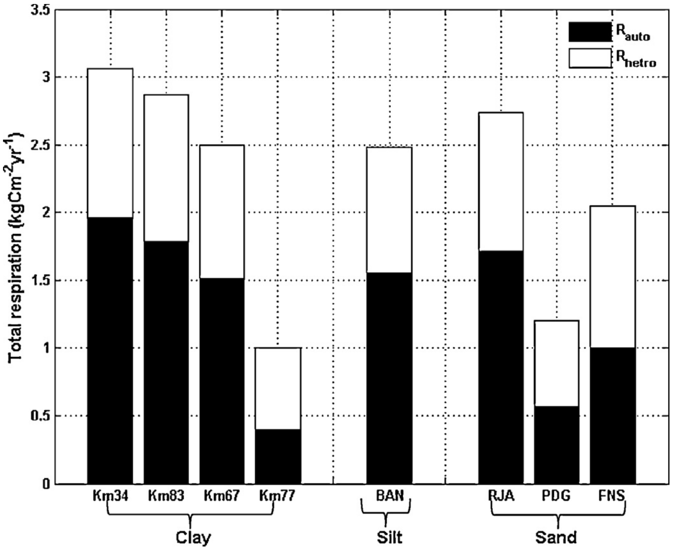

Fig. 5. Component of total respiration for each site in kg C m^{-2} yr^{-1} grouped with respect to soil types.

Table 5
ISAM estimated leaf litter (Kg C m^{-2} yr^{-1}) for the LBA sites reported as the mean for the study sites flux measurement period.

Leaf litter		
	ISAM	measurements
Km34	0.3	0.25 ± 0.35[a]
Km67	0.3	0.4[b]
Km83	0.3	0.3[c]
RJA	0.3	–
BAN	0.3	–
PDG	0.2	–
FNS	0.2	0.1–0.2[d]
Km77	0.1	–

[a] Measurement is the average of the three estimates from Luizão et al. (2004).
[b] Measurement taken from Rice et al. (2004).
[c] Measurement taken from Hirsch et al. (2004).
[d] Measurement taken from Trumbore et al. (1995).

related to the difference in the LAI (maximum LAI for the FNS is 5.7 m^2 m^{-2} compared to 3.2 m^2 m^{-2} for the Km77 site) (data provided by the LBA core team), which is related to the nutrient and soil moisture availability (Sakai et al., 2004). For the sites with no reported measurements (RJA, BAN, and PDG sites), we could not draw any conclusions as to whether the model is overestimating or underestimating leaf litter.

4. Discussion

We use the ISAM to simulate the carbon fluxes and carbon pools in the vegetation and the soils for eight LBA sites representative of three different biome types (forest, savanna, and pasture). The ISAM estimates for GPP are well within the uncertainty range of the site measurements.

GPP for the FNS pasture site is higher than the Km77 pasture site. One explanation for this difference is that the soil in the Eastern Amazon, the region where Km77 is located, is believed to have lower soil nutrients than the soils in the Western Amazon, the regions for FNS location (Asner et al., 1999). Moreover, de Moraes et al. (1996) and Dias-Filho et al. (2001) studies suggest that pasture growth is limited by nutrient availability, such as phosphorus, calcium and potassium. Studies also suggest that soil moisture stress at Km77 is higher during the dry season due to shallow roots (Sakai et al., 2004). It is interesting to note that the ISAM is able to track down productivity for these two diverse pasture sites (FNS and Km77), because the ISAM is able to account for water and nutrient limitations under the variable environmental conditions.

To investigate whether the LBA sites acted as a net source or sink for atmospheric CO_2, NEE is calculated as the difference between NPP and R_{hetro}. The model results indicate that all the forest sites are net sink of carbon, while the savanna (PDG) and pasture (FNS) sites are neutral and only Km77 is net source of carbon. Based on the model results, the Km67 has accumulated more carbon and hence this site acted as carbon sink, which is evident from the fact that the estimated and measured NPP for this site are higher compared to the other LBA forest sites. Pyle et al. (2008) suggests that this site has possibly experienced mortality in the 1990s and re-growing thin younger forest have absorbed more carbon (Figueira et al., 2008). Based on our model results and measurements, our assumption is that this site has been occupied by the younger or smaller trees with higher NPP/GPP ratio (Delucia et al., 2007) and lower R_{auto} compared to the other forest sites. We account for the disturbances for Km67 site by reducing the modeled vegetation carbon by 20% at the beginning of the model simulation year. The NPP for the disturbed case is 1.4 Kg C m^{-2} yr^{-1} (Table 4), which is compared well with the measured data and about 50% higher than without disturbance case. In addition, the underestimation of the modeled leaf litter for the Km67 site could be related to the mortality hypothesis for the Km67 site associated with drought stress and that could have caused an increase in the observed leaf litter.

The measurement for the Km67 site suggests that this site is net source for carbon (Malhi et al., 2009), while our model results show the opposite because the model underestimated soil respiration. The model result suggests that the Km34 site acted as net sink for carbon. Our model results agree with the site ecophysiological measurements, but disagree with the site flux measurements (Malhi et al., 2009) (Table 2). Because of the large uncertainties in the site measurements, particularly for R_{leaf} and R_{hetro} (Malhi et al., 2009; Ryan and Law, 2005; Suseela et al., 2012), and the difference in the measurements results based on the two measurements methods (ecophysiological and eddy flux covariance), it is difficult to correctly evaluate the model NEE estimates and therefore the role of the ecosystem as a carbon sink or source.

The total ecosystem respiration, R_{total}, for the tropical evergreen sites decreases with decreasing precipitation during the dry season because soil respiration is constrained by desiccation (Saleska et al., 2003). Both Km34 and RJA sites have the same dry season length (3 months), but the dry season precipitation for the Km34 site (35 cm) is 40% larger than the RJA site (25 cm). R_{total} for the Km34 is 15% higher than the RJA site, which indicates that R_{total} is driven by dry season precipitation amount and not by dry season length. Therefore, the respond of R_{total} to climate change will be dependent on the severity of the dry season and the wet season length.

While land surface models suffers from the inability to accurately estimate soil carbon, ISAM soil carbon estimates for the Amazonian sites are in close agreement with the site measurements (within 4.5%). Indeed, the strength of the ISAM is in its ability to accurately calculate soil carbon dynamics, which is important for predicting its role in climate change as soil respiration is expected to increase due to increase in soil temperature (Raich and Schlesinger, 1992; Rustard et al., 2002). It will be advantageous to have long term measurements of soil carbon to have a better insight of the interannual dynamics of this carbon pool since tropical soils are suggested to have a potential to sequester an additional amount of carbon (Lal, 2002, 2004).

The annual total magnitude of the ISAM leaf litter estimates are close to the site estimates. However, when compared with leaf litter estimates from Rice et al. (2004), the seasonal variations do not match (not shown). The ISAM litter production do not show seasonal variability for the Km67 site because leaf litter is controlled by cold temperature and water stress and the cold temperature stress will not have an effect on leaf litter for tropical sites (Arora and Boer, 2005). Based on the ISAM, the water stress factor for the Km67 site is almost uniform throughout the season and the current litter production scheme has failed to capture the seasonality of leaf litter for tropical evergreen sites (this is the case of the majority of land surface models). We will address this issue in the future studies by modifying the ISAM litter production model to account for the seasonal variation in LAI when estimating leaf litter, in such a way that leaf litter should increase with a decrease in LAI and vice versa.

The improvement introduced to the carbon allocation and autotrophic respiration schemes are interconnected, because R_{auto} is dependent on the vegetation carbon pool size. By adjusting the parameters for the vegetation turnover rates, we are able to improve the model estimated total vegetation biomass (Table 2). Furthermore, model assumes different maintenance respiration rates for the different vegetation pools and for different biomes. These modifications are introduced to be consistent with studies showing that leaf maintenance respiration rate is higher than the stem and the roots (Ryan et al., 1996). To our knowledge, these implementations are unique to ISAM and help to improve the model performance as evident from the model results (Table 4).

5. Conclusion

We show that by calibrating the ISAM using site data for the LBA sites, the results compare well with the site measurements and within their uncertainty range. The ISAM is calibrated using data for the Km34 tropical forest site and tested for the other four topical forest sites included in the LBA project. Also, ISAM is calibrated for the one pasture site (FNS) and validated for the other pasture site (Km77). The ISAM is calibrated for the savanna site (PDG), but could not be further validated due to lack of data availability. The ISAM estimated results for the measured sites compare well with the site measurements thus validating our calibration techniques. Despite the limitation in the site measurements and data availability, it can be concluded that global land surface models can be improved substantially by integrating site level data.

In this application of the ISAM, we revise and modify the autotrophic respiration and the carbon allocation schemes, which proved successful as evident from model results. We believe that these modified schemes and calibrated parameters can be implemented in other land surface models depending on their model structure to improve their estimates. We learn from this analysis that several improvement for ISAM are needed to enhance the model capability for the global simulations, such as adding more biome to represent heterogeneity in landscapes (e.g. woody savanna), and improving the litter production schemes for tropical forests to better capture the seasonal variability in the leaf litter. Furthermore, leaf litter seasonality can be improved by adjusting the seasonality of the leaf carbon pool through the modification of the carbon allocation parameters and accounting the impacts of light stress on these parameters, specifically for in tropical evergreen forests, Finally, LAI is the main driver for the leaf litter seasonality, and we plan to introduce dynamic LAI schemes to ISAM to improve the LAI seasonality.

Acknowledgments

We thank the scientists who collected tower observations during field campaigns under the LBA project, funded by NASA, the Brazilian Ministry of Science and Technology and European Agencies. We also thank the LBA-Data-Model-Intercomparison project funded by NASA's Terrestrial Ecology Program (grant NNX09AL52G), which provided the datasets that made this work possible. The ISAM development work presented here is supported by the National Aeronautics and Space Administration (NASA) Land Cover and Land Use Change Program (No. NNX08AK75G) and the Office of Science (BER), U.S. Department of Energy (DOE-DE-SC0006706).

Appendix A.

Table A1
Model parameter values used in this study.

Function		Units	Tropical evergreen forest	Savanna	Pasture	Reference
Structure	Veg_frct	–	1	0.80[a]	0.85[a]	This study
	cn_{leaf}	–	42	25	50	White et al. (2000)
	cn_{stem}	–	300	200	200	White et al. (2000)
	cn_{root}	–	58	50	50	White et al. (2000)
Photosynthesis	V_{cmax}	$\mu mole\ m^{-2}\ s^{-1}$	95	94	84	Domingues et al. (2007)
	k_n	–	0.5	0.5	0.5	Arora and Boer (2005)
Plant respiration	k_{leaf}	$gCg\ N^{-1} d^{-1}$	0.09[a]	0.04[a]	0.06[a]	This study
	k_{stem}	$gCg\ N^{-1} d^{-1}$	0.01[a]	0.04[a]	0[a]	This study
	k_{root}	$gCg\ N^{-1} d^{-1}$	0.04[a]	0.06[a]	0.06[a]	This study
Phenology	daylen	h	12	12	12	This study
	bio_tr	°C	12	12	11	This study
	Bio_trmin	°C	7	2	2	This study
	LAI_max	$m^{-2}\ m^{-1-2}$	6	4.50	3.29	This study
Allocation	ω	–	0.6	0.8	0.5	This study
	ε_{leaf}	–	0.5[a]	0.4	0.4	This study
	ε_{stem}	–	0.001[a]	0	0	This study
	ε_{root}	–	0.499[a]	0.60	0.60	This study
	k	–	1.6	1.6	1.6	Arora and Boer (2005)
Litter production	Y_{leaf}	years	2	0.75	1	This study
	r_{wmax}	d^{-1}	0.005	0.005	0.005	Arora and Boer (2005)
	r_{tmax}	d^{-1}	0.20	0.30	0.15	This study
	b_w	–	3.0	3.0	3.0	Arora and Boer (2005)
	b_t	–	3.0	3.0	3.0	Arora and Boer (2005)
	T_{cold}	°C	5.0	5.0	5.0	Arora and Boer (2005)
Turnover rate	Y_{stem}	years	50[a]	2.5	1.0	This study
	Y_{froot}/Y_{croot}	years	2.0/8.0[a]	2.0/5.0	1.0/2.0	This study

[a] Calibrated parameters.

Table A2
ISAM equations for the carbon modules.

Function	Equations		Reference
Plant autotrophic respiration	$R_{leaf} = k_{leaf} \times \frac{C_{leaf}}{cn_{leaf}} \times \varnothing \times gt$	(S1)	Sitch et al. (2003), Arora (2003)
	$R_{stem} = k_{stem} \times \frac{C_{stem}}{cn_{stem}} \times gt$	(S2)	
	$R_{root} = k_{root} \times \frac{C_{root}}{cn_{root}} \times \varnothing \times gt$	(S3)	
	$Q_{10} = 3.22 - 0.046 \times T_{veg}$ for leaves and stems	(S4)	
	$Q_{10} = 3.22 - 0.046 \times T_{soil}$ for roots	(S5)	
	$gt = Q_{10}^{(T_{veg}-20)/10}$ for leaves and stems	(S6)	

Table A2 (*Continued*)

Function	Equations	Reference
	$gt = Q_{10}^{(T_{\text{soil}}-20)/10}$ for roots (S7)	
	$R_{\text{mtotal}} = R_{\text{leaf}} + R_{\text{stem}} + R_{\text{root}}$ (S8)	
	$R_G = 0.25 \times \max(0, \text{GPP} - R_{\text{mtotal}})$ (S9)	
	$R_{\text{auto}} = R_{\text{mtotal}} + R_G$ (S10)	
Phenology	For deciduous trees:	
	$\text{leaf onset} = \left\{ \begin{array}{c} \text{julian day} > 200 \\ \text{day length} > \text{daylen} \\ T_r > \text{bio\_tr} \\ \\ \text{GPP} - R_{\text{leaf}} > 0 \end{array} \right.$ (S11)	
	$\text{normal growth} = \{\text{LAI} \geq (0.5 \times \text{LAI\_max})$ (S12)	
	$\text{leaf fall} = \left\{ \begin{array}{c} \text{julian day} > 200 \\ \text{day length} > \text{daylen} \\ T_r < \text{bio\_trmin} \\ \text{or} \\ \text{GPP} - R_{\text{leaf}} > 0 \end{array} \ \Big\vert\ \text{or LAI} < (0.4 \times \text{LAI\_max}) \right\}$	
	$\text{dormant.no leaf} = \left\{ \begin{array}{c} \text{day length} < \text{daylen} \\ T_r < \text{bio\_trmin} \end{array} \right.$ (S14)	
	For herbaceous:	
	$\text{leaf onset} = \left\{ \begin{array}{c} \text{GPP} - R_{\text{leaf}} > 0 \\ \\ T_r > 275 \end{array} \right.$ (S15)	
	$\text{normal growth} = \{\text{LAI} > (0.5 \times \text{LAI\_max})$ (S16)	
	$\text{leaf fall} = \left\{ \begin{array}{c} \text{GPP} - R_{\text{leaf}} < 0 \\ \\ T_r < 275 \\ \\ \text{ws} < 0.4 \end{array} \right.$ (S17)	
Allocation	$\text{NPP} = \text{GPP} - R_{\text{mtotal}} - R_G$ (S18)	Arora and Boer (2005), Friedlingstein et al. (1999)
	For tropical evergreen forest:	
	If NPP > 0:	
	$C_{\text{leaf}} = \text{NPP} \times \text{Allo\_fact}_{\text{leaf}}$ (S19)	
	$C_{\text{stem}} = \text{NPP} \times \text{Allo\_fact}_{\text{stem}}$ (S20)	
	$C_{\text{roots}} = \text{NPP} \times \text{Allo\_fact}_{\text{roots}}$ (S21)	
	If NPP < 0:	
	$C_{\text{leaf}} = \text{GPP} \times \text{Allo\_fact}_{\text{leaf}} - R_{\text{leaf}}$ (S22)	
	$C_{\text{stem}} = \text{GPP} \times \text{Allo\_fact}_{\text{stem}} - R_{\text{stem}}$ (S23)	
	$C_{\text{roots}} = \text{GPP} \times \text{Allo\_fact}_{\text{root}} - R_{\text{root}}$ (S24)	
	For savanna and pasture:	
	Maximum growth:	
	$C_{\text{leaf}} = \text{NPP}$ (S25)	
	Normal growth:	
	Same as tropical forest	
	Leaf off	
	$C_{\text{leaf}} = (\text{GPP} - R_G - R_{\text{leaf}}) \times \text{Allo\_fact}_{\text{leaf}} - R_{\text{leaf}}$ (S26)	
	$C_{\text{stem}} = (\text{GPP} - R_G - R_{\text{stem}}) \times \text{Allo\_fact}_{\text{stem}} - R_{\text{stem}}$ (S27)	
	$C_{\text{root}} = (\text{GPP} - R_G - R_{\text{root}}) \times \text{Allo\_fact}_{\text{root}} - R_{\text{root}}$ (S28)	
	Allocation factor for trees:	
	$\text{Allo\_fact}_{\text{stem}} = \dfrac{\varepsilon_{\text{stem}} + \omega(1-L)}{1+\omega(2-L-ws)}$ (S29)	
	$\text{Allo\_fact}_{\text{root}} = \dfrac{\varepsilon_{\text{root}} + \omega(1-ws)}{1+\omega(2-L-ws)}$ (S30)	
	$\text{Allo\_fact}_{\text{leaf}} = 1 - \text{Allo\_fact}_{\text{stem}} - \text{allo\_fact}_{\text{root}}$ (S31)	
	Allocation factor for herbaceous:	
	$\text{Allo\_fact}_{\text{root}} = \dfrac{\varepsilon_{\text{root}} + \omega(1-ws)}{1+\omega(1+L-ws)}$ (S32)	
	$\text{Allo\_fact}_{\text{leaf}} = \dfrac{\varepsilon_{\text{leaf}} + \omega L}{1+\omega(1+L-ws)}$ (S33)	
	$L = \left\{ \begin{array}{l} \exp(-k_n \times \text{LAI}) \quad \text{for trees and crops} \\ \\ \max\left(0, \dfrac{1-\text{LAI}}{4.5}\right) \quad \text{for grasses} \end{array} \right.$ (S34)	
Litter production	$\text{Litter\_prod}_{\text{leaf}} = C_{\text{leaf}} \times (r_n + r_w + r_t)$ (S35)	Arora and Boer (2005)
	$r_n = \dfrac{1}{(Y_{\text{leaf}} \times 365)}$ (S36)	
	$r_w = r_{w\,\max} \times (1-ws)^{b_w}$ (S37)	
	$r_t = r_{t\,\max} \times (1-\beta_t)^{b_t}$ (S38)	
	$\beta_t = \left\{ \begin{array}{ll} 1 & T_{\text{air}} > T_{\text{cold}} \\ \dfrac{(T_{\text{air}} - (T_{\text{cold}} - 5.0))}{5.0} & T_{\text{cold}} > T_{\text{air}} > (T_{\text{cold}} - 5.0) \\ 0 & T_{\text{air}} \leq (T_{\text{cold}} - 5.0) \end{array} \right.$	
	For stems and roots:	
	$\text{Litter\_prod}_{\text{stem}} = C_{\text{stem}} \times \left(\dfrac{1}{Y_{\text{stem}} \times 365}\right)$ (S40)	
	$\text{Litter\_prod}_{\text{root}} = C_{\text{root}} \times \left(\dfrac{1}{Y_{\text{root}} \times 365}\right)$ (S41)	

References

Amthor, J.S., 1984. The role of maintenance respiration in plant growth. Plant Cell Envion. 7, 561–569.

Amthor, J.S., 2000. The McCree-de Wit-Penning de Vries-Thornley Respiration Paradigms: 30 years later. Ann. Bot. 86, 1–20.

Andreae, M.O., Artaxo, P., Brandão, C., Carswell, F.E., Ciccioli, P., da Costa, A.L., Culf, A.D., Esteves, L.J., Gash, J.H.C., Grace, J., Kabat, P., Lelieveld, J., Malhi, Y., Manzi, A.O., Meixner, F.X., Nobre, A.D., Nobre, C., Ruivo, M.d.L.P., Silva-Dias, M.A., Stefani, P., Valentini, R., von Jouanne, J., Waterloo, M.J., 2002. Biogeochemical cycling of carbon, water, energy, trace gases, and aerosols in Amazonia: the LBA-EUSTACH experiments. J. Geophys. Res. 107, http://dx.doi.org/10.1029/2001JD000524.

Arora, V.K., 2003. Simulating energy and carbon fluxes over winter wheat using coupled land surface and terrestrial ecosystem models. Agric. Forenst Meteorol. 118, 21–47.

Arora, V.K., Boer, G.J., 2005. A parameterization of leaf phenology for the terrestrial ecosystem component of climate models. Global Change Biol. 11, 39–59.

Araújo, A.C., Nobre, A.D., Kruijt, B., Elbers, A., Dallorosa, R., Stefani, P., von Randow, C., Manazi, A.O., Culf, A.D., Gash, J.H.C., Valentini, R., Kabat, P., 2002. Comparative measurements of carbon dioxide fluxes from two nearby towers in a central Amazonian rainforest: the Manaus LBA site. J. Geophys. Res. 107, http://dx.doi.org/10.1029/2001JD000676.

Asner, G.P., Townsend, A.R., Bustamante, M.M.C., 1999. Spectrometry of pasture condition and biogeochemistry in Central Amazon. Geophys. Res. Lett. 26 (17), 2769–2772.

Asner, G.P., Townsend, A.R., Braswell, B.H., 2000. Satellite observation of El Nifio effects on Amazon forest phenology and productivity. Geophys. Res. Lett. 27 (7), 981–984.

Asner, G.P., Knapp, D.E., Broadbent, E.N., Oliveria, P.J.C., Keller, M., Silva, J.N., 2005. Selective logging in the Brazilian Amazon. Science 310, 480–482.

Avissar, R., Nobre, C.A., 2002. Preface to special issue on the Large-Scale Biosphere-Atmosphere experiment in Amazonia (LBA). J. Geophys. Res. 107 (D21), http://dx.doi.org/10.1029/2002JD002507.

Avissar, R., Silva Dias, P.L., Silva Dias, M.A.F., Nobre, C., 2002. The large-scale biosphere atmosphere experiment in Amazonia (LBA): insights and future research needs. J. Geophys. Res. 107, http://dx.doi.org/10.1029/2002JD002704.

Ball, J.T., Woodrow, I.E., Berry, J.A., 1987. A model predicting stomatal conductance and its contribution to the control of photosynthesis under different environmental conditions. In: Biggens, J. (Ed.), Progress in Photosynthesis Research, vol. V. Martinus Nijhoff, Dordrecht, pp. 221–224.

Baker, I.T., Prihodko, L., Denning, A.S., Goulden, M., Miller, S., Da Rocha, H.R., 2008. Seasonal drought stress in the Amazon: reconciling models and observations. J. Geophys. Res. 113 (G00B01), http://dx.doi.org/10.1029/2007JG000644.

Beer, C., Reichstein, M., Tomelleri, E., Ciais, P., Jung, M., Carvalhais, N., Rödenbeck, C., Arain, M.A., Baldocchi, D., Bonan, G.B., Bondeau, A., Cescatti, A., Lasslop, G., Lindroth, A., Lomas, M., Luyssaert, S., Margolis, H., Oleson, K.W., Roupsard, O., Veenendaal, E., Viovy, N., Williams, C., Woodward, F.I., Papale, D., 2010. Terrestrial gross carbon uptake: global distribution and covariation with climate. Science 329, 834–838.

Botta, A., Ramankutty, N., Foley, J.A., 2002. Long-term variations of climate and carbon fluxes over the Amazon basin. Geophys. Res. Lett. 29 (9), 1319.

Borma, L.S., da Rocha, H.R., Cabral, O.M., von Randow, C., Collicchio, E., Kurzatowski, D., Brugger, P.J., Freitas, H., Tannus, R., Oliveira, L., Renńo, C.D., Artaxo, P., 2009. Atmosphere and hydrological controls of the evapotranspiration over a floodplain forest in the Bananal Island region, Amazonia. J. Geophys. Res. 114, http://dx.doi.org/10.1029/2007JG000641.

Costa, M.H., Foley, J.A., 2000. Combined effects of deforestation and doubled atmospheric CO_2 concentration on the climate of Amazonia. J. Climate 13, 18–34.

Concilio, A., Ma, S., Ryu, S.R., North, M., Chen, J., 2006. Soil respiration response to experimental disturbance over 3 years. Forest Ecol. Manage. 228, 82–90.

Collatz, G.J., Ball, T.J., Grivet, C., Berry, J.A., 1991. Physiological and environmental regulations of stomatal conductance, photosynthesis and transpiration: a model that included a laminar boundary layer. Agric. Forest Meteorol. 54, 107–136.

Collatz, G.J., Ribas-Carbo, M., Berry, J.A., 1992. Coupled photosynthesis-stomatal conductance model for leaves of C4 plants. Aust. J. Plant Physiol. 19, 519–538.

Dai, Y., Dickenson, R.E., Wang, Y.-P., 2004. A two-big-leaf model for canopy temperature, photosynthesis, and stomatal conductance. J. Climate 17, 2281–2299.

Da Rocha, H.R., Freitas, H.C., Rosolen, R., Juárez, R.I.N., Tannus, R.N., Ligo, M.A., Cabral, O.M.R., Silva Dias, M.A.F., 2002. Measurements of CO exchange over a woodland savanna 2 (Cerrado Sensu stricto) in southeast Brasil. Biota Neotrop. 2, 1–11.

Da Rocha, H.R., Goulden, M.L., Miller, S.D., Menton, M.C., Pinto, L.D.V.O., de Frettas, H.C., Silva Figueira, A.M.E., 2004. Seasonality of water and heat fluxes over a tropical forest in eastern Amazonia. Ecol. Appl. 14 (4), S22–S32.

Davidson, E.A., De Araújo, A.C., Artaxo, P., Balch, J.K., Brown, I.F., Bustamante, M.M.C., Coe1, M.T., DeFries, R.S., Keller, M., Longo, M., Munger, J.W., Schroeder, W., Soares-Filho, B.S., Souza Jr., C.M., Wofsy, S.C., 2012. The Amazonian basin in transition. Nature 481, 321–328.

De Castro, E.A., Kaufman, J.B., 1998. Ecosystem structure in the Brazilian Cerrado: a vegetation gradient of aboveground biomass, root mass and consumption by fire. J. Trop. Ecol. 14, 263–283.

De carvahlo Conceição Telles, E., de Camargo, P.B., Martinelli, L.A., Trumbore, S.E., de costa, E.S., Santos, J., Higuchi, N., Oliverira, R.C., 2003. Influence of soil texture on carbon dynamic and storage potential in tropical forest sites of Amazonia. Global Biogeochem. Cycles 17 (2), http://dx.doi.org/10.1029/2002GB001953.

de Gonçalves, L.G.G., Borak, J.S., Costa, M.N., Saleska, S.R., Baker, I., Restrepo-Coupe, N., Muza, M.N., 2012. Overview of the large-scale biosphere-atmosphere experiment in Amazônia Data Model Intercomparison Project (LBA-DMIP). Agric. Forest Meteorol., http://dx.doi.org/10.1016/j.agrformet.2013.03.011, in press.

de Moraes, J.F.L., Volkoff, B., Cerri, C.C., Bernoux, M., 1996. Soil properties under Amazon forest and changes due to the pasture installation in Rondoˆnia, Brazil. Geoderma 70, 63–81.

Dias-Filho, M.B., Davidson, E.A., de Carvalho, C.J.R., 2001. Linking Biogeochemical cycles to cattle pasture management and sustainability in the Amazon basin. In: McClain, M.E., Richey, R.L.J.E. (Eds.), The Biogeochemistry of the Amazon Basin. Oxford University Press, New York, pp. 84–105.

Delucia, E.J., frake, J.E., Thomas, R.B., Conzales-Meler, M., 2007. Forest carbon use efficiency: is respiration a constant fraction of gross primary production? Global Change Biol. 13, 1157–1167.

Domingues, T.F., Martinelli, L.A., Ehleringer, J.R., 2007. Ecophysiological traits of plant functional groups in forest and pasture ecosystems from eastern Amazonia. Brazil. Plant Ecol. 193, 101–112.

Farquhar, G.D., von Caemmerer, S., Berry, J.A., 1980. A biochemical model of photosynthetic CO_2 assimilation in leaves of C3 species. Planta 149, 78–90.

Figueira, A.M.S., Miller, S.D., de Sousa, C.A.D., Menton, M.C., Maia, A.R., da Rocha, H.R., Goulden, M.L., 2008. Effects of selective logging on tropical forest tree growth. J. Geophys. Res. 113, http://dx.doi.org/10.1029/2007JG000577.

Fishers, M.J., Rao, I.M., Ayarza, M.A., Lascano, C.E., Sanz, J.I., Thomas, R.J., Vera, R.R., 1994. Carbon storage by introduced deep-rooted grasses in the South American savannas. Nature 371, 236–238.

Foley, J.A., Prentice, I.C., Ramankutty, P., Levis, S., Pollard, D., Sitch, S., Haxeltine, A., 1996. An integrated biosphere model of land surface processes, terrestrial carbon balance, and vegetation dynamics. Global Biogeochem. Cycles 10 (4), 603–628.

Foley, J.A., Botta, A., Coe, M.T., Costa, M.H., 2002. El Niño–Southern oscillation and the climate, ecosystems and rivers of Amazonia. Global Biogeochem. Cycles 16 (4), http://dx.doi.org/10.1029/2002GB001872.1132.

Foley, J.A., Asner, G.P., Costa, N.H., Coe, M.T., DeFries, R., Gibbs, H.K., Howard, E.A., Olsen, S., Patz, J., Ramankutty, P., Synder, P., 2007. Amazonia revealed: forest degradation and loss of ecosystem goods and services in the Amazonian basin. Font. Ecol. Environ. 5 (1), 25–32.

Friedlingstein, P., Joel, G., Field, C.B., Fung, I.Y., 1999. Toward an allocation scheme for global terrestrial carbon models. Global Change Biol. 5, 755–770.

Grace, J., Jośe, J.S., Meir, P., Miranda, H.S., Montes, R.A., 2006. Productivity and carbon fluxes of tropical savannas. J. Biogeogr. 33, 387–400.

Hirsch, A.I., Little, W.S., Houghton, R.A., Scott, N.A., White, J.D., 2004. The net carbon flux due to deforestation and forest re-growth in the Brazilian Amazon: analysis using a process-based model. Global Change Biol. 10, 908–924.

Hollinger, D.Y., Richardson, A.D., 2005. Uncertainty in eddy covariance measurements and its application to physiological models. Tree Physiol. 25, 873–885.

Huntzinger, D.N., Post, W.M., Wei, Y., Michalak, A.M., West, T.O., Jacobson, A.R., Baker, I.T., Chen, J.M., Davis, K.J., Hayes, D.J., Hoffman, F.M., Jain, A.K., Liu, S., McGuire, A.D., Neilson, R.P., Potter, C., Poulter, B., Price, D., Raczka, B.M., Tian, H.Q., Thornton, P., Tomelleri, E., Viovy, N., Xiao, J., Yuan, W., Zeng, N., Zhao, M., Cook, R., 2012. North American Carbon Program (NCAP) regional interim synthesis: terrestrial biosphere model intercomparison. Ecol. Model. 232, 144–157.

Houghton, R.A., Skole, D.L., Nobre, C.A., Hackler, J.L., Lawrence, K.T., Chomentowski, W.H., 2000. Annual fluxes of carbon from deforestation and regrowth in the Brazilian Amazon. Nature 403, 301–304.

Houghton, R.A., Lawrence, K.T., Hackler, J.L., Brown, S., 2001. The spatial distribution of forest biomass in Brazilian Amazon: a comparison of estimates. Global Change Biol. 7, 731–746.

Hutyra, L.R., Munger, J.W., Saleska, S.R., Gottlieb, E., Daube, B.C., Dunn, A.L., Amaral, D.F., de Camargo, P., Wodsy, S.C., 2007. Seasonal controls on the exchange of carbon and water in an Amazonian rain forest. J. Geophys. Res. 112, http://dx.doi.org/10.1029/2006JG000365.

Jain, A.K., Kheshgi, H.S., Wuebbles, D.J., 1996. A globally aggregated reconstruction of cycles of carbon and its isotopes, Tellus. Ser. B. 48 (4), 583–600, http://dx.doi.org/10.1034/j.1600-0889.1996.t01-1-00012.x.

Jain, A.K., Yang, X., 2005. Modeling the effects of two different land cover change data sets on the carbon stocks of plants and soils in concert with CO2 and climate change. Global Biogeochem. Cycles 19 (GB2015), http://dx.doi.org/10.1029/2004GB002349.

Jain, A.K., Tao, Z., Yang, X., Gillespie, C., 2006. Estimates of global biomass burning emissions for reactive greenhouse gases (CO, NMHCs, and NOx) and CO_2. J. Geophys. Res. 111, D06304, http://dx.doi.org/10.1029/2005JD006237.

Jain, A.K., Yang, X., Kheshgi, H., McGuire, A.D., Post, W., Kicklighter, D., 2009. Nitrogen attenuation of terrestrial carbon cycle response to global environmental factors. Global Biogeochem. Cycles 23, http://dx.doi.org/10.1029/2009GB003519.

Keller, M., Varner, R., Dias, J.D., Silva, H., 2005. Soil–atmosphere exchange of nitrous oxide, nitric oxide, methane, and carbon dioxide in logged and undisturbed forest in the Tapajos National Forest, Brazil. Earth Interac. 9, 1–23.

Keenan, T.F., Baker, I., Barr, A., Ciais, P., Davis, K., Dietze, M., Dragoni, D., Gough, C.M., Grant, R., Hollinger, D., Hufkens, K., Poulter, B., Mccaughey, H., Raczka, B., Ryu, Y., Schaefer, K., Tian, H., Verbeeck, H., Zhao, M., Richardson, A.D., 2012. Terrestrial biosphere model performance for inter-annual variability of land-atmosphere CO2 exchange. Global Change Biol. 18, 1971–1987.

Laurance, W.F., Cochrane, M.A., Bergen, S., Fearnside, P.M., Delamonica, P., Barber, C., D'Angelo, S., Fernandes, T., 2001. Environment – the future of the Brazilian Amazon. Science 291, 438–439.

Lawrence, D., Oleson, K.W., Flanner, M.G., Thorton, P.E., Swenson, S.C., Lawrence, P.L., Zeng, X., Yang, Z-L., Levis, S., Skaguchi, K., Bonan, G.B., Slater, A.G., 2011: Parameterization improvements and functional and structural advances in version 4 of the community land model. J. Adv. Model. Earth Syst. 3, M03001, 27 pp., http://dx.doi.org/10.1029/2011MS000045

Lal, R., 2002. The potential of soils of the tropics to sequester carbon and mitigate the greenhouse effect. Agronomy 76, 1–30.

Lal, R., 2004. Soil carbon sequestration to mitigate climate change. Geoderma 123, 1–22.

Luizão, R.C.C., Luizão, F.J., Paiva, R.Q., Monteiro, T.F., Sousa, L.S., Kruijt, B., 2004. Variation of carbon and nitrogen cycling processes along a topographic gradient in a central Amazonian forest. Global Change Biol. 10, 592–600.

Malhi, Y., Grace, J., 2000. Tropical forests and atmospheric carbon dioxide. Tree 15 (8), 332–337.

Malhi, Y., Baker, T.R., Phillips, O.L., Almeida, S., Alvarez, E., Arroyo, L., Chave, J., Czimczik, C.I., Di Fiore, A., Higuchizz, N., Killeen, T.J., Laurance, S.G., Laurance, W.F., Lewisz, S.L., Marcado Montoya, L.M., Monteagudo, A., Neill, D.A., Núñez Vargas, P., Patiño, S., Pitman, N.A., Quesada, C.A., Salomão, R., Silva, J.N.M., Torres Lezama, A., Martínez, R.V., Terborgh, J., Vinceti, B., Lloyd, J., 2004. The aboveground coarse wood productivity of 104 Neotropical forest plots. Global Change Biol. 10, 563–591.

Malhi, Y., Roberts, J.T., Betts, R.A., Killeen, T.J., Li, W., Nobre, C.A., 2008. Climate change, deforestation, and the fate of the Amazon. Science 319, 169–172.

Malhi, Y., Aragáo, L.E.O.C., Metcalfe, D.B., Paiva, R., Quesada, C.A., Almeida, S., Anserson, L., Brando, P., Chmabers, J.Q., da Costa, A.C., Hutyra, L.R., Oliveira, P., Patiño, S., Pyle, E., Roberstson, A., Teixeira, L.M., 2009. Comprehensive assessment of carbon productivity, allocation and storage in three Amazonian forests. Global Change Biol., http://dx.doi.org/10.1111/j.1365-2486.2008.01780.x.

Malhi, Y., Doughty, C., Galbraith, D., 2011. The allocation of ecosystem net primary productivity in tropical forests. Philos. Trans. Roy. Soc. B. 366, 3225–3245.

McGuire, A.D., Melillo, J., Joyce, L., Kicklighter, D., Grace, A., Moore III, B., Vorosmarty, C., 1992. Interactions between carbon and nitrogen dynamics in estimating net primary productivity for potential vegetation in North America. Global Biogeochem. Cycles 6 (2), 101–124, http://dx.doi.org/10.1029/92GB00219.

Meiyappan, P., Jain, A.K., 2012. Three distinct global estimates of historic land-cover change and land-use conversions for over 200 years. Front. Earth Sci., http://dx.doi.org/10.1007/s11707-012-0314-2.

Miller, S.D., Goulden, M.L., Menton, M.C., da Rocha, H.R., de Freitas, H.C., Silva Figueira, A.M.E., Dias de Sousa, C.A., 2004. Biometric and micrometerological measurements of tropical forest carbon balance. Ecol. Appl. 14, S114–S126.

Melillo, J.M., Houghton, R.A., Kicklighter, D.W., McGuire, A.D., 1996. Tropical deforestation and the global carbon budget. Annu. Rev. Energy Environ. 21, 293–310.

Moran, E.F., 1993. Deforestation and land use in Brazilian Amazon. Human Ecol. 21 (1), 1–21.

Mortan, D.C., DeFries, R., Shimabukuro, Y.E., Anderson, L.O., Del Bon Espírito-Santos, F., Hansen, M., Carrol, M., 2005. Rapid assessment of annual deforestation in Brazilian amazon using MODIS data. Earth Interac. 9 (8), 1–22.

Oleson, K.W., Niu, G.-Y., Yang, Z.-L., Lawrence, D.M., Thornton, P.E., Lawrence, P.J., Stöckli, S., Dickenson, R.E., Bonan, G.B., Levis, S., Dai, A., Qian, T., 2008. Improvements to the community land model and their impact on the hydrological cycle. J. Geophys. Res. 113 (G01021), http://dx.doi.org/10.1029/2007JG000563.

Potter, C., Klooster, S., de Carvalho, C.R., Genovese, V.B., Torregrosa, A., Dungan, J., Bobo, M., Coughlan, J., 2001. Modeling seasonal and interannual variability in ecosystem carbon cycling for the Brazilian Amazon region. J. Geophys. Res. 106 (D10), 10423–10466.

Potter, C., Klooster, S., Huete, A., Genovese, V., Bustamante, M., Ferreira, L.G., De Oliveira Junior, R., Zepp, R., 2009. Terrestrial carbon sinks in the Brazilian Amazon and Cerrado region predicted from MODIS satellite data and ecosystem modeling. Biogeosci. Discuss. 6, 947–969.

Poulter, B., Hattermann, F., Hawkins, E., Zaehle, Z., Sitch, S., Restrope-Coupe, N., Heyder, U., Cramer, W., 2010. Robust dynamics of amazon dieback to climate change with perturbed ecosystem model parameters. Global Change Biol. 16, 2476–2495.

Prentice, C., Farquhar, G., Fasham, M., Goulden, M., Heimann, M., Jaramillo, V., Kheshgi, H., Que're', C.L., Scholes, R., Wallace, D., 2001. The carbon cycle and atmospheric CO_2. In: Houghton, J.T., et al. (Eds.), Climate Change 2001: The Scientific Basis: Contribution of WGI to the Third Assessment Report of the IPCC. Cambridge Univ. Press, New York, pp. 183–237.

Pyle, E.H., Santoni, G.W., Nascimento, H.E.M., Hutyra, L.R., Vieira, S., Curran, D.J., can Haren, J., Saleska, S.R., Chow, V.Y., Carmago, P.B., Laurance, W.F., Wofsy, S.C., 2008. Dynamics of carbon, biomass, and structure in two Amazonian forests. J. Geophys. Res. 113 (G00B08), http://dx.doi.org/10.1029/2007JG000592.

Ramankutty, N., Gibbs, H.K., Achard, F., Defries, R., Foley, J.A., Houghton, R.A., 2007. Challenges to estimating carbon emissions from tropical deforestation. Global Change Biol. 13 (51–66), http://dx.doi.org/10.1111/j.1365-2486.2006.01272.x.

Richardson, A.D., Anderson, R.S., Arain, M.A., Barr, A.G., Bohrer, G., Chen, G., Chen, J.M., Ciais, P., Davis, K.J., Desai, A.R., Dietze, M.C., Dragoni, D., Garrity, S.R., Gough, C.M., Grant, R., Hollinger, D.Y., Margolis, H.A., McCaughey, H., Migliavacca, M., Monson, R.K., Munger, J.W., Poulter, B., Raczka, B.M., Ricciuto, D.M., Sahoo, A.K., Schaefer, K., Tian, H., Vargas, R., Verbeeck, H., Xiao, J., Xue, Y., 2012. Terrestrial biosphere models need better representation of vegetation phenology: results from the North American Carbon Program Site Synthesis. Global Change Biol. 18, 566–584.

Rice, A.H., Pyle, E.H., Saleska, S.R., Hutyra, L., Palace, M., Keller, M., de Camargo, P.B., Portilho, K., Marques, D.F., Wofsy, S.C., 2004. Carbon balance and vegetation dynamic in an old-growth Amazonian forest. Ecol. Appl. 14 (4), S55–S71.

Raich, J.W., Schlesinger, W.H., 1992. The global carbon dioxide flux in soil respiration and its relationship to vegetation and climate. Tellus 44B, 81–99.

Rustard, L.E., Huntington, T.G., Boone, R.D., 2002. Controls on soil respiration: implications for climate change. Biogeochemistry 48, 1–6.

Ryan, M.G., Gower, S.T., Hubbard, R.M., Warning, R.H., Gholz, H.L., Cropper Jr., W.D., Running, S.W., 1995. Woody tissue maintenance respiration for four conifers in contrasting climates. Oecologia 101, 133–140.

Ryan, M.G., Hubbard, R.M., Pongracic, S., Raison, R.J., McMurtrie, R.E., 1996. Foliage, fine-root, woody-tissue, and stand respiration in *Pinus radiata* in relation to nitrogen status. Tree Physiol. 16, 333–343.

Ryan, M.G., Law, B.E., 2005. Interpreting, measuring, and modeling soil respiration. Biogeochemistry 73, 3–27.

Sakai, R.K., Fitzjarrald, D.R., Moraes, O.L.L., Staebler, R.M., Acevedo, O.C., Czikowsky, M.J., da Silva, R., Brait, E., Miranda, V., 2004. Land-use change effects on local energy, water, and carbon balances in an Amazonian agricultural field. Global Change Biol. 10, 895–907.

Saleska, S.R., Miller, S.D., Matross, D.M., Goulden, M.L., Wofsy, S.C., da Rocha, H.R., de Camargo, P.B., Crill, P., Daube, B.C., de Freitas, H.C., Hutyra, L., Keller, M., Kirckhoff, V., Menton, M., Munger, L.W., Pyle, E.H., Rice, A.H., Silva, H., 2003. Carbon in Amazon forests: unexpected seasonal fluxes and disturbance-induced losses. Science 302, 1554–1557.

Schaefer, K., Schwalm, C.R., Williams, C., Arain, M.A., Barr, A., Chen, J.M., Davis, K.J., Dimitrov, D., Hilton, T.W., Hollinger, D.Y., Humphreys, E., Poulter, B., Raczka, B.M., Richardson, A.D., Sahoo, A., Thornton, P., Vargas, R., Verbeeck, H., Anderson, R., Baker, I., Black, T.A., Bolstad, P., Chen, J., Curtis, P.S., Desai, A.R., Dietze, M., Dragoni, D., Gough, C., Grant, R.F., Gu, L., Jain, A., Kucharik, C., Law, B., Liu, S., Lokipitiya, E., Margolis, H.A., Matamala, R., McCaughey, J.H., Monson, R., Munger, J.W., Oechel, W., Peng, C., Price, D.T., Ricciuto, D., Riley, W.J., Roulet, N., Tian, H., Tonitto, C., Torn, M., Weng, E., Zhou, X., 2012. A model-data comparison of gross primary productivity: results from the North American Carbon Program site synthesis. J. Geophys. Res. 117 (G3), 2156–2202.

Schimel, D.S., Braswell, B., McKeown, R., Ojima, D., Parton, W., Pulliam, W., 1996. Climate and nitrogen controls on the geography and timescales of terrestrial biogeochemical cycling. Global Biogeochem. Cycles 10, 677–692, http://dx.doi.org/10.1029/96GB01524.

Sitch, S., Smith, B., Prentice, I.C., Arneth, A., Bondeau, A., Cramer, W., Kaplan, J.O., Levis, S., Lucht, W., Sykes, M.T., Thonicke, K., Venevsky, S., 2003. Evaluation of ecosystem dynamics, plant geography and terrestrial carbon cycling in the LPJ dynamic global vegetation model. Global Change Biol. 9, 161–185.

Skole, D., Tucker, C., 1993. Tropical deforestation and habitat fragmentation in the Amazon: satellite data from 1978 to 1988. Science 260, 1905–1910.

Song, Y., Jain, A.K., McIsaac, G.F., 2013. Implementation of dynamic crop growth processes into a land surface model: evaluation of energy, water and carbon fluxes under corn and soybean rotation. Biogeosciences, submitted for publication.

Suseela, V., Conant, R.T., Wallenstein, M.D., Dukes, J.S., 2012. Effects of soil moisture on the temperature sensitivity of heterotrophic respiration vary seasonally in an old-field climate change experiment. Global Change Biol. 18, 336–348.

Tian, H.Q., Melillo, J.M., Kicklighter, D.W., McGuire, A.D., Helfrich, J.V.K., Moore, B., Vorosmarty, C.J., 1998. Effect of interannual climate variability on carbon storage in Amazonian ecosystems. Nature 396, 664–667.

Trumbore, S.E., Davidson, E.A., de Camargo, P.B., Nepstad, D.C., Martinelli, L.A., 1995. Belowground cycling of carbon in forests an pastures of Eastern Amazonia. Global Biogeochem. Cycles 9 (4), 515–528.

Vargas, R., Allen, M.F., 2008. Diel patterns of soil respiration in a tropical forest after Hurricane Wilma. J. Geophys. Res. 113, http://dx.doi.org/10.1029/2007JG000620.

Von Randow, C., Manzi, O., Kruijt, B., de Oliveira, P.J., Zanchi, F.B., Silva, E.L., Hodnett, M.G., Gash, J.H.C., Elbers, J.A., Waterloo, M.J., Cardoso, E.L., Kabat, P., 2004. Comparative measurements and seasonal variations in energy and carbon exchange over forest and pasture in South West Amazonia. Theor. Appl. Climatol. 78, 5–26.

Werth, D., Avissar, R., 2002. The local and global effects of Amazon deforestation. J. Geophys. Res. 17, http://dx.doi.org/10.1029/2001JD000717.

White, M.A., Thornton, P.E., Running, S.W., 1997. A continental phenology model for monitoring vegetation responses to interannual climate variability. Global Biogeochem. Cycles 11 (2), 217–234.

White, M.A., Thornton, P.E., Running, S.W., Nemani, R.R., 2000. Parameterization and sensitivity analysis of the Biome-BGC terrestrial ecosystem model: net primary production controls. Earth Interact. 4, 1–85.

Wilson, K., Goldstein, A., Falge, E., Aubinet, M., Baldocchi, D., Berbigier, P., Bernhofer, C., Ceulemans, R., Dolman, H., Field, C., Grelle, A., Ibrom, A., Law, B.E., Kowalski, A., Meyers, T., Moncrieff, J., Monson, R., Oechel, W., Tenhunen, J., Valentini, R., Verma, S., 2002. Energy balance closure at FLUXNET sites. Agric. Forest Meteorol. 113, 223–243.

Yang, X., Wittig, V., Jain, A.K., Post, W.M., 2009. Integration of nitrogen cycle dynamics into the Integrated Science Assessment Model for the study of terrestrial ecosystem responses to global change. Global Biogeochem. Cycles 23 (GB4029), http://dx.doi.org/10.1029/2009GB003474.

Zhang, Y., Xu, M., Chen, H., Adams, J., 2009. Global patterns of NPP to GPP ratio derived from MODIS data: effects of ecosystem type, geographical location and climate. Global Ecol. Biogeogr. 18, 280–290.